PAPER

NJC
www.rsc.org/njc

Complexation behaviour of hexadentate ligands possessing N_2O_4 and $N_2O_2S_2$ cores: differential reactivity towards Co(II), Ni(II) and Zn(II) salts and structures of the products

Gudneppanavar Rajsekhar,[a] **Chebrolu P. Rao,***[a] **Pauli Saarenketo,**[b]
Kalle Nättinen[b] **and Kari Rissanen**[b]

[a] *Bioinorganic Laboratory, Department of Chemistry, Indian Institute of Technology Bombay, Mumbai 400 076, India. E-mail: cprao@chem.iitb.ac.in*
[b] *Department of Chemistry, University of Jyvaskyla, Jyvaskyla SF - 40351, Finland*

***Received** (in Montpellier, France) 8th May 2003, Accepted 9th September 2003*
First published as an Advance Article on the web 30th October 2003

Reactions of divalent metal salts of Co, Ni and Zn with 1,2-di(salicylaldimino-*o*-phenylthio)ethane (H_2L^1) and 1,2-di(naphthaldimino-*o*-phenylthio)ethane (H_2L^2), having $N_2O_2S_2$ cores, and 1,2-di(*O*-salicylaldimino-*o*-hydroxyphenyl)ethane (H_2L^3), having a N_2O_4 core, have been explored. Out of the three ligands and the nine products obtained from the corresponding reactions, two ligands and seven products were crystallographically characterized. However, all the ligands and the products were characterized by analytical and spectral methods. Reaction of H_2L^1 and H_2L^2 with Co(II) salts results in oxidative cleavage of the C–S bond to produce a Co(III) product bound to two dissimilar tridentate ligands formed as a result of the cleavage. The reaction of H_2L^1 and H_2L^2 with Co(III)acac in the presence of methanolic NaOH also shows cleavage of the C–S bond to give compounds similar to those obtained by reacting H_2L^1 and H_2L^2 with Co(II) salts in the absence of additional external base. However, the reaction of Co(II) salt with H_2L^3 did not lead to any C–O bond cleavage; rather it produced an octahedral Co(II) complex of the hexadentate H_2L^3. Reactions of all these three ligands with Ni(II) salt resulted in octahedral complexes of the corresponding hexadentate ligands. In the case of Zn(II), while H_2L^3 with a N_2O_4 core resulted in an octahedral complex, H_2L^1 and H_2L^2, both with a $N_2O_2S_2$ core, produced pseudo-octahedral complexes whose Zn–S bond lengths are rather long. The conformations of both the 5-membered and 6-membered chelate rings formed in the products were evaluated. The extent of distortion exhibited in the geometry of these octahedral complexes was computed and appropriately compared.

Introduction

Molecules possessing O, N and S donor sites are important in the development of coordination chemistry as well as in the bio-mimetic chemistry of a number of metal ions, particularly the transition metals. Among these, non-cyclic hexadentate ligands with N_2O_4 and $N_2O_2S_2$ binding cores are well-suited for the coordination of transition metal ions with a high preference towards the later ones.[1] A non-cyclic ligand of the $N_2O_2S_2$ type, 1,2-di(salicylaldimino-*o*-phenylthio)ethane (H_2L^1), generated interesting chemistry with oxidative cleavage of the ligand when it was reacted with a Co(II) salt, rather than forming a simple complex.[2] However, an earlier work reported the formation of only a simple cobalt complex from the same reaction but the product was not subjected to NMR or X-ray studies.[3] C–S bond cleavage is not an unusual phenomenon, particularly with cobalt group elements in the presence of cyclic thioether ligands as well as with some non-cyclic ones,[4] but this is not the case for the ligands in this paper. In the literature,[4] the suitable size for the cleavage of thia-chelates was addressed and in such cases the C–H bond is activated by a base, such as Et_3N or NaOH/KOH. The present study differs even in this context. All these points aroused great interest in our group to understand what happens to the cleavage reaction when (a) the sulfur is replaced by oxygen, (b) Co(II) is replaced by Ni(II) or Zn(II), (c) the counter ion of the Co(II) salt is varied and (d) Co(II) is replaced by a Co(III) salt. These aspects were addressed in a systematic manner by developing three types of hexadentate ligands (H_2L^1, H_2L^2 and H_2L^3), having either an N_2O_4 core or an $N_2O_2S_2$ core, and studying their reactivity and coordination chemistry using three divalent metal ions, *viz.*, Co(II), Ni(II) and Zn(II) and four different Co(II) salts as well as one acetylacetonate (acac) compound of Co(III). In the process, the reaction product in each case was isolated, purified and characterized. Structures of several of these products, including the precursor ligands, were established by single crystal X-ray diffraction (XRD). The results of all these studies are reported in this paper in a comparative way.

DOI: 10.1039/b305313j

Results and discussion

All the compounds reported in Scheme 1, except those of Ni(II) (**2**, **5** and **8**), were characterized by ^1H and ^{13}C NMR and all were characterized by FAB-MS, UV-Vis and magnetic moment measurements. Except for H_2L^2, **4** and **2**, all other ligands and complexes were structurally characterized by single crystal XRD.

1. Reactions of H_2L^1–H_2L^3 with Co(II)

While the reaction of Co(II) salts (acetate, chloride, sulfate and acetylacetonate) with H_2L^1 or H_2L^2 having an $N_2O_2S_2$ core results in the oxidative cleavage of the C–S bond, the reaction of H_2L^3 having an N_2O_4 core produces only a simple Co(II) complex.

C–S bond cleavage with H_2L^1 and H_2L^2. The reactions of H_2L^1 or H_2L^2 with Co(acetate)$_2$·$4H_2O$ in a 1:1 ratio in

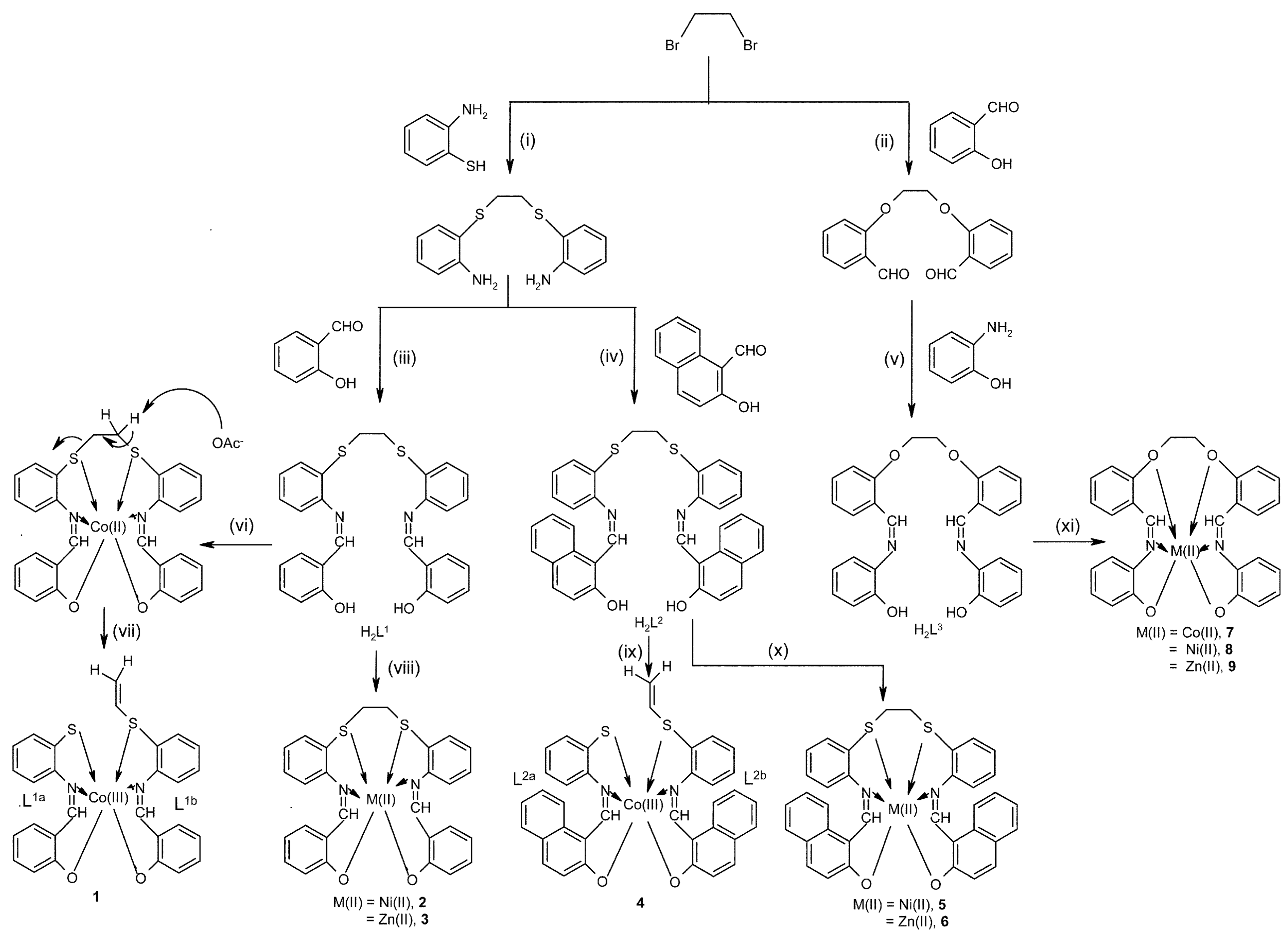

Scheme 1 Schematic representation of the synthesis of the ligands and their Co(III), Co(II), Ni(II) and Zn(II) complexes. (i) Dry ethanol and Na; (ii) aqueous NaOH; (iii) MeOH, RT, stirring; (iv) MeOH, RT, stirring; (v) EtOH, reflux for 6 h; (vi) $Co(OAc)_2{\cdot}4H_2O$, argon/$Co(acac)_3$/NaOH; (vii) oxygen; (viii) $Ni(OAc)_2{\cdot}4H_2O$/$Zn(OAc)_2{\cdot}2H_2O$; (ix) $Co(OAc)_2{\cdot}4H_2O$, argon, oxygen/$Co(acac)_3$, NaOH; (x) $Ni(OAc)_2{\cdot}4H_2O$/$Zn(OAc)_2{\cdot}2H_2O$; (xi) $Co(OAc)_2{\cdot}4H_2O$/$Ni(OAc)_2{\cdot}4H_2O$/$Zn(OAc)_2{\cdot}2H_2O$.

dichloromethane–methanol yielded [Co(III)(L^{1a})(L^{1b})] (**1**) and [Co(III)(L^{2a})(L^{2b})] (**4**), respectively. In both the cases the ligands H_2L^1 and H_2L^2 are cleaved at a C–S bond to result in two non-equivalent parts, *viz.*, L^{1a} and L^{1b} or L^{2a} and L^{2b}, and these in turn are still bound to the Co(III) center as tridentate ligands, as shown in Scheme 1.

The reactions were initially allowed to proceed under Ar atmosphere and later on under O_2. During this process, the reaction mixture goes through a color change from orange-red to dark brown. The reaction of H_2L^1 with Co(acetate)$_2{\cdot}$4H_2O was monitored in solution by UV-Vis absorption spectra as a function of time. It was noticed that when the reaction mixture was maintained under Ar atmosphere, the orange-red complex remains stable, but when the reaction was purged with O_2, it quickly converted to a dark brown Co(III) complex with cleavage of H_2L^1 as shown in Scheme 1. Thus, under Ar atmosphere the reaction mixture exhibited a ligand → metal charge transfer band at 425 nm in the absorption spectra and this band was found to grow in intensity as a function of time; this peak is reminiscent of a Co(II) center. When the reaction mixture was bubbled with O_2, the spectra exhibited a very broad band, which upon de-convolution represents two least resolved bands positioned at 440 and 475 nm, respectively, with almost equal absorbance, indicating the formation of a more positive Co(III) center, favoring a better charge transfer from the thiolate moiety that was generated by cleavage (L^{1a}). Similarly, the band observed at 300 nm under Ar atmosphere shifts to 285 nm when purged with O_2. Even the absorption spectrum measured from the dichloromethane solution of the isolated product exhibited a spectrum that is exactly identical to that obtained from the reaction mixture after O_2 purging. Similarly, in the case of **4** the absorption spectrum measured from the isolated product exhibited a broad band, which upon de-convolution represents two less resolved bands positioned at 480 and 510 nm.

From the FTIR spectra of **1** and **4**, it was possible to deduce the binding of the $-O^-_{\text{phenolate}}$ group owing to the disappearance of the corresponding ν_{OH} vibration that is otherwise present in the precursor ligand spectra. Involvement of the –C=N– moiety in binding the metal ion center is evident based on the shift (8–20 cm^{-1}) observed in the stretching frequency of this group in the complexes. Both the complexes exhibited a strong $\nu_{C=C}$ vibration arising from the $-S-HC{=}CH_2$ moiety formed as a result of the C–S bond cleavage in L^1 and L^2 at 1525 and 1532 cm^{-1}, respectively. The molecular weights of the ligands as well as the complexes were confirmed based on the molecular ion peaks observed in their respective FAB mass spectra. The results are consistent with mononuclear complexes. Both the complexes were found to be diamagnetic from their magnetic susceptibility measurements, supporting the +3 oxidation state of the cobalt.

Molecular structure of H_2L^1. H_2L^1crystallizes in the monoclinic system with $P2_1/c$ space group. The molecule sits on a crystallographic center of symmetry and hence each asymmetric unit cell possesses two halves of the molecule. The molecule exhibits an 'S'-like structure. Such a molecular structure is stabilized *via* the presence of a strong intramolecular 6-atom O–H···N type interaction between the phenolic–O–H and the –N=C– moieties and another weak intramolecular 9-atom O–H···S type interaction between the phenolic–O–H and the $Ph-S-CH_2-$ moieties.

Crystal structure of **1** *and the role of the anion of the Co(II) salt.* The crystal structure of the reaction product, [Co(III)-(L^{1a})(L^{1b})] (**1**) shown in Fig. 1 reveals the presence of two ligands, *viz.*, L^{1a} (dianionic) and L^{1b} (monoanionic), formed upon cleavage of a C–S bond, both acting as tridentate ligands by extending the ONS binding core. This results in the formation of two 5-membered and two 6-membered chelate rings to give a distorted octahedral $Co(ONS)_2$ core. The conformations of the various chelates present in the complex are shown in the Table 1. The octahedral coordination geometry is much less distorted compared with the regular octahedron geometry as shown by the observed narrower bite angles, 88.3(1)°–95.8(1)°, and the *trans* angles: 175.6(1)°, 175.6(1)° and 177.9(2)°. Selected bond lengths are given in Table 2 and the bond angles in Table 3. The metric data is fully supported by the cleavage of H_2L^1 in order to form the ethylene moiety C17b=C18b (1.302 Å) and Co–$S_{\textbf{thiolate}}$ (2.227 Å) and Co–$S_{\textbf{thioether}}$ (2.238 Å) bonds. No abnormal bond lengths were observed in the structure.

A similar reaction carried out with another salt of Co(II), $CoCl_2{\cdot}6H_2O$, and H_2L^1 resulted in a product whose composition and crystal structure were found to be the same as that of [Co(III)(L^{1a})(L^{1b})]. Based on FAB mass and ^{1}H NMR studies, it was found that the reaction carried out using $Co(SO_4)_2{\cdot}7H_2O$ and $Co(acac)_2{\cdot}2H_2O$ also resulted in the same product and thereby exhibited C–S bond cleavage. Thus, in these four cases the final product was found to be same, irrespective of the anion of the Co(II) salt used.

^{1}H and ^{13}C NMR studies. The absence of paramagnetic shifts in the ^{1}H NMR spectrum of **4** supports the presence of a Co(III) center formed by the oxidation of Co(II). XRD supports the Co being present in its 3+ state as well as the presence of the C–S bond-cleaved fragments (L^{1a} and L^{1b}) bound to the metal ion center as reported in this paper. This was further supported by the ^{1}H NMR spectrum of **1**. The spectrum of **4** also clearly supports the formation of two ligands, L^{2a} and L^{2b}, formed by the cleavage of a C–S bond in the reaction between Co(II) acetate and H_2L^2: the imine proton peaks are doubled and new signals from vinylic protons arise, as shown in Fig. 2(a). The same information is also revealed through the spectral changes observed in case of the aromatic protons. These features are vividly highlighted when the spectrum of **4** is compared with that of the precursor ligand, H_2L^2, given in Fig. 2(b). The peak observed at 3.195 ppm due to the bridging $-S-CH_2-CH_2-S-$ moiety in H_2L^2 disappears in the spectrum of **4** and two new multiplets appear in the region of 5.574–5.957 ppm, which are due to the vinyl protons ($-S-C\boldsymbol{H}=C\boldsymbol{H}_2$), the assignment of which is made using ^{1}H–^{1}H COSY as shown by the cross peak in Fig. 3(a). Based on the ^{1}H–^{13}C HMQC experiments [Fig. 3(b)], the ^{13}C peaks observed at 128.8 and 126.9 ppm were assigned to S–$\boldsymbol{C}$H = CH_2 and –S–CH=$\boldsymbol{C}H_2$, respectively. The peak doubling for imine protons was further confirmed through the ^{1}H–^{13}C HMQC experiment shown in Fig. 3(a).

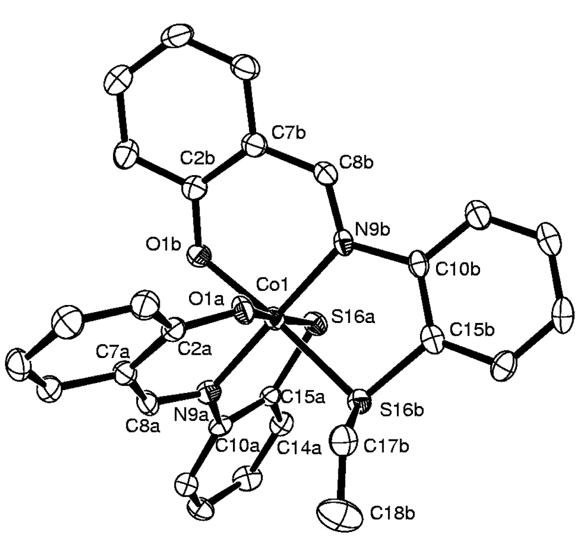

Fig. 1 Molecular structure with atom labeling for **1**.

Table 1 Conformation of the chelates present in the complexes **1**, **7**, **5**, **8**, **3**, **6** and **9**

Complex	Chelate	Conformation[a]
1	Co1–N9a–C10a–C15a–S16a	C_s
	Co1–S16b–C15b–C10b–N9b	C_2
	Co1–O1b–C2b–C7b–C8b–N9b	Skew boat
	Co1–O1a–C2a–C7a–C8a–N9a	Boat
7	Co18–N8–C7–C2–O1	C_s
	Co18–O16–C17–C17_2–O16_2	A
	Co18–N8–C9–C10–C15–O16	Skew boat
5	Ni1–S23–C22–C21–S20	C_2
	Ni1–S20–C19–C14–N13	C_s
	Ni1–S23–C24–C29–N30	C_2
	Ni1–N30–C31–C32–C41–O42	Skew boat
	Ni1–N13–C12–C11–C2–O1	Boat
8	Ni18–O1–C2–C7–N8	C_s
	Ni18–O16–C17–C17_2–O16_2	A
	Ni18–N8–C9–C10–C15–O16	Skew boat
3	Zn1–S16–C17–C18–S19	C_2
	Zn1–S16–C15–C10–N9	C_2
	Zn1–S19–C20–C25–N26	C_s
	Zn1–N26–C27–C28–C33–O34	Skew boat
	Zn1–N9–C8–C7–C2–O1	Skew boat
6	Zn1–S20–C21–C21_2–S20_2	A
	Zn1–S20–C19–C14–N13	C_s
	Zn1–N13–C12–C11–C2–O1	Skew boat
9	Zn18–O1–C2–C7–N8	C_2
	Zn18–N8–C9–C10–C15–O16	Skew boat
	Zn18–O16–C17–C17_2–O16_2	A

[a] C_2 = half-chair form; C_s = envelop form; A = planar

Non-cleavage of the C–O bond in H_2L^3. Unlike the reactions of $H_2L^1$and H_2L^2, the reaction of H_2L^3 with $Co(acetate)_2{\cdot}4H_2O$ in a 1:1 ratio in dichloromethane–methanol yielded [Co(L^3)] (**7**) with no cleavage of the C–O bond (Scheme 1). The elemental compositions of H_2L^3 and [Co(L^3)] yielded satisfactory results. The peak at 3423 cm^{-1} due to ν_{OH} in the FTIR spectrum of $H_2L^3$was found to disappear in the spectrum of **7** and furthermore the peak due to $\nu_{CH=N}$ was shifted from 1619 cm^{-1} in the ligand to 1598 cm^{-1} in the complex, indicating the binding of cobalt through $-O^-$ and CH=N, respectively. The spectrum of crystals of **7** exhibited $\nu_{C=O}$ at 1700 cm^{-1} and two sharp peaks for ν_{CH} at 2924 and 2853 cm^{-1}. When these crystals were crushed, washed with diethyl ether and dried *in vacuo*, the peaks at 1700, 2924 and 2853 cm^{-1} disappeared, indicating the loss of acetic acid otherwise present in the lattice. The molecular weight of H_2L^3 and [Co(L^3)] were confirmed based on their FAB mass spectra. The observed magnetic moment value for **7** (μ_{obs} = 4.899 BM) arises from the cobalt in its +2 oxidation state along with orbital contribution expected to arise from a high-spin d^7 system. In the ^{1}H NMR spectrum of the ligand, H_2L^3, only the peaks arising from one-half of the molecule were observed owing to the symmetry. On the other hand, the ^{1}H NMR spectrum of **7** exhibited paramagnetically shifted bands in the region −25 to +25 ppm.

Molecular structure of H_2L^3 and **7**. Both the structures of H_2L^3 and **7** possess a center of symmetry and have only one-half of the molecule in their asymmetric unit cells. The ORTEP plots

Table 2 Selected bond distances (Å) in the primary coordination sphere of complexes **1, 3, 5, 6, 7, 8** and **9**

Bond	[Co(III)(L^{1a})(L^{1b})] (**1**)	[Co(L^3)]·CH_3COOH (**7**)[a]	[Ni(L^2)]·0.5CH_3OH (**5**)	[Ni(L^3)]·CH_3COOH (**8**)[a]	[Zn(L^1)] (**3**)	[Zn(L^2)] (**6**)[a]	[Zn(L^3)]·CH_3OH (**9**)[a]
M–N	1.913(3)	2.066(2)	2.028(3)	2.018(4)	2.095(3)	2.073(2)	2.151(2)
	1.926(2)		2.028(3)		2.101(4)		
M–$O_{phenolate}$	1.894(2)	2.007(2)	2.008(3)	2.010(4)	1.980(3)	1.978(2)	2.020(2)
	1.914(2)		2.014(3)		2.009(3)		
M–O_{ether}	–	2.217(2)	–	2.178(3)	–	–	2.328(2)
M–S_{ether}	2.227(1)	–	2.413(2)	–	2.582(2)	2.692(1)	–
	2.238(1)		2.459(2)		2.675(2)		

[a] Molecule possessing a center of symmetry.

of H_2L^3 and **7** are shown in Figs. 4 and 5, respectively. The molecule of H_2L^3 is folded due to one C–H···O (5-atom) type intramolecular hydrogen bond interaction present between the –CH=N– and the Ph–O–CH_2– moieties and one O–H···N (5-atom) type interaction present between the phenolic–O–H and the –CH=N– moieties. In the structure of **7**, the cobalt is present in a distorted octahedral geometry bound through two phenolic moieties, two imine moieties and two ether oxygens, resulting in a neutral mononuclear complex with a Co(II)–N_2O_4 core. Thus, the X-ray structure clearly shows an intact C–O bond and supports the specificity of Co(II) salts towards the cleavage of C–S bonds rather than the C–O bond. Among the coordinating atoms the imine nitrogens occupy axial positions and the remaining four oxygen atoms occupy the equatorial positions. The octahedral geometry is more distorted than the regular octahedron geometry as shown by their wider range of bite angles, 75.0(1)° to 112.5(2)°, and *trans* angles, 155.7(1)° and 179.5(2)°. The conformations of the chelates found in **7** are given in Table 1. Selected bond lengths and bond angles are given in Tables 2 and 3, respectively. However, no abnormalities were found with the bond length data of H_2L^3 and **7**. The M–N and M–$O_{phenolate}$ distances observed in **7** with Co(II) are considerably longer, by about 0.15 and 0.10 Å, respectively, when compared with similar bond lengths observed in the structure of **1** with Co(III), due to the difference in the oxidation states.

2. Reactions of H_2L^1 and H_2L^2 with Co(III)

Reactions of H_2L^1 and H_2L^2 with Co(acac)$_3$ in 1 : 1 ratio at room temperature as well as under reflux conditions in dichloromethane–methanol did not yield any products. But the same reactions, when carried out in the presence of 2 equiv. of methanolic NaOH, resulted in the formation of **1** and **4**, respectively, as confirmed by ^1H NMR studies. Thus, the alkali activates the thioether group while deprotonating the phenolic –OH groups. This observation is in agreement with that reported in the literature.[4i]

3. Reaction of H_2L^1–H_2L^3 with Ni(II)

Reactions of H_2L^1–H_2L^3 with Ni(CH_3COO)$_2$·4H_2O resulted in the formation of the hexacoordinated Ni(II) complexes **2**, **5** and **8**, respectively, as shown in Scheme 1. In none of these final products were either the C–S or the C–O bonds broken upon reaction with Ni(II) salt, though C–S bond cleavage was reported in the literature in the case of a thioether complex of nickel.[4j] Thus, Ni(II) behaves quite differently from Co(II), where the latter is stabilized in the +3 oxidation state when cleaving the C–S bond with H_2L^1 and H_2L^2, while with H_2L^3 the final product is in the same +2 oxidation state and the C–O bond is intact. In the FTIR spectra of **2**, **5** and **8** the observed decrease in $\nu_{CH=N}$ (8–19 cm^{-1}) and the

Table 3 Selected bond angles (°) in the coordination sphere of complexes **1, 3, 5, 6, 7, 8** and **9**

	[Co(III)(L^{1a})(L^{1b})] (**1**)	[Co(L^3)]·CH_3COOH (**7**)	[Ni(L^2)]·0.5CH_3OH (**5**)	[Ni(L^3)]·CH_3COOH (**8**)	[Zn(L^1)] (**3**)	[Zn(L^2)] (**6**)	[Zn(L^3)]·CH_3OH (**9**)
O_{phe}–M–$O_{phe.}$	87.89(9)	112.53(12)	93.67(12)	106.0(2)	104.25(13)	103.01(11)	111.57(11)
O_{phe}–M–N	84.93(10)	81.99(9)	88.45(13)	96.11(16)	91.82(12)	88.33(8)	82.75(8)
	95.81(10)	98.26(9)	90.28(13)	82.78(16)	99.45(13)	100.22(8)	104.07(8)
	95.23(10)		89.49(13)		96.68(12)		
	86.25(10)		88.33(13)		90.07(12)		
O_{phe}–M–S	175.64(7)[a]	–	90.38(10)	–	168.21(10)	162.82(5)	–
	92.28(7)[a]		170.90(9)		86.03(9)	89.35(6)	
	94.07(7)[b]		170.62(9)		90.50(9)		
	175.64(7)[b]		90.23(8)		162.64(9)		
O_{phe}–M–O_{ether}	–	155.66(8)	–	161.37(14)	–	–	88.75(8)
		88.30(8)		89.29(14)			156.60(7)
N–M–S	90.72(8)[a]	–	97.98(11)	–	80.66(10)	77.63(6)	–
	89.13(8)[b]		83.55(11)		88.94(10)	91.94(6)	
	88.25(8)[b]		82.99(9)		89.01(10)		
	89.69(8)[b]		99.17(10)		78.99(10)		
N–M–O_{ether}	–	82.65(9)	–	96.41(15)	–	–	89.43(8)
		96.99(9)		85.02(15)			81.04(8)
N–M–N	177.94(12)	179.54(14)	177.44(14)	178.2(2)	165.31(13)	166.33(11)	168.06(12)
S–M–S	86.07(3)	–	87.02(4)	–	80.38(4)	81.38(3)	–
O_{ether}–M–O_{ether}	–	74.96(10)	–	78.12(18)	–	–	74.35(10)

[a] Co(III) bound to thioether. [b] Co(III) bound to thiolate.

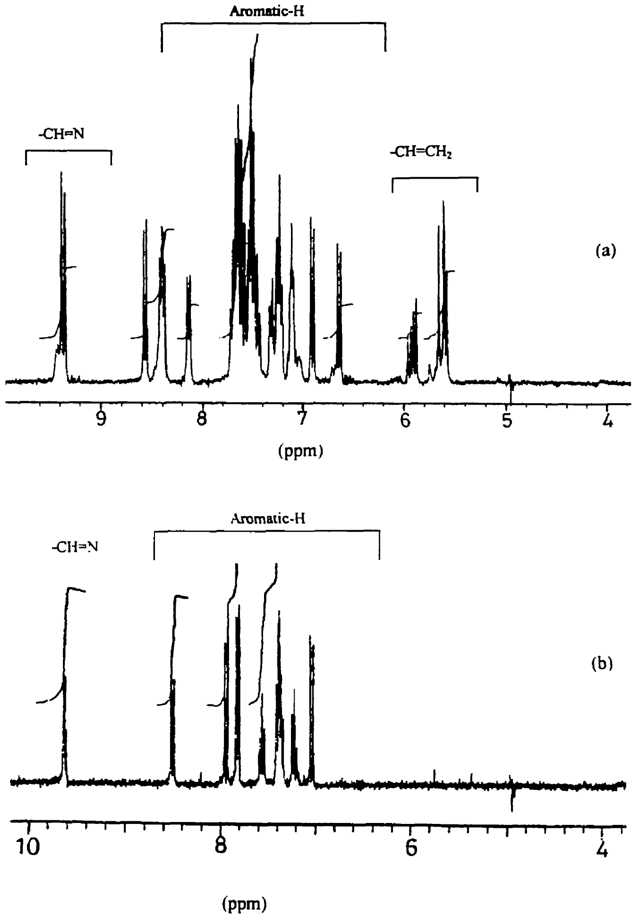

Fig. 2 ^{1}H-NMR spectra in DMSO-d$_6$ of (a) complex **4** and (b) ligand H_2L^2.

disappearance of ν_{OH} vibrations support the binding through –O$^-$ and –CH=N– moieties. The analytical and FAB mass data fits with the mononuclear complexes shown in Scheme 1. The experimental magnetic moments were found to be 2.841, 3.049 and 2.812 BM, respectively, for **2**, **5** and **8** at room temperature. The ^{1}H NMR spectra of these complexes exhibited broad and shifted bands due to their paramagnetic nature, as supported by the magnetic moments. In the absorption spectra of the Ni(II) complexes **2**, **5** and **8**, bands corresponding to $^3A_{2g} \rightarrow {}^3T_{1g}(F)$ and $^3A_{2g} \rightarrow {}^3T_{1g}(P)$ transitions are observed at 567–624 and 445–471 nm, respectively, and a third band due to $^3A_{2g} \rightarrow {}^3T_{2g}$ at 879–908 nm supports the octahedral geometry around the Ni(II) center.

Molecular structures of 5 and 8. The crystal structures of both complexes **5** and **8** showed a distorted octahedral geometry around the Ni(II) center, in which Ni(II) is bound through the $N_2O_2S_2$ core in **5** and the N_2O_4 core in **8**; both the corresponding ligands act as hexadentate ones. The asymmetric unit cell in **8** contains half of the molecule due to the center of symmetry. In **5**, the asymmetric unit contains one molecule of the complex and half a methanol molecule. The molecular structure of **5** is shown in Fig. 6. In the structures of **5** and **8**, both the nitrogens are disposed *trans* to each other. The observed distortion in the geometry around the Ni(II) center in **5** is less than that observed in **8** as judged based on the spread of the bite angles [83.0(1)°–98.0(1)°] and the *trans* angles [170.6(1)°, 170.9(1)° and 177.4(2)°] in the case of **5**, while these are 78.1(2)–106.0(2)° and 161.4(2)°, 161.4(2)° and 178.2(2)°, respectively, for **8**. In both the nickel complexes, the nickel(II) exhibits five chelates, of which three are five-membered and two are six-membered ones (Table 1). The selected bond lengths are given in Table 2 and the selected bond angles are given in Table 3.

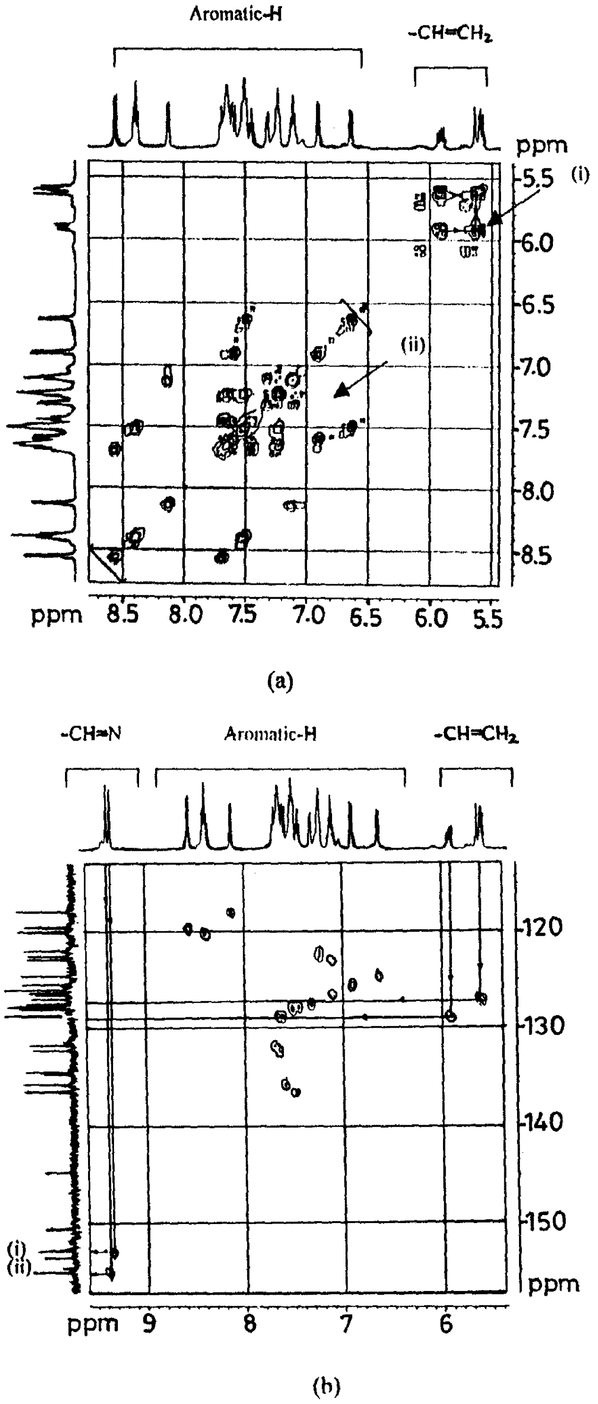

Fig. 3 (a) ^{1}H–^{1}H HMQC spectrum of **4**: (i) represents cross peak corresponds to the coupling of (–C*H* = CH$_2$) and (–CH = C*H*$_2$) protons, (ii) represents cross peaks due to aromatic protons. (b) ^{1}H–^{13}C HMQC spectrum of **4**: (i) and (ii) correspond to the carbon resonances of two different –CH=N groups.

Hydrogen bonding in 5 and 8. In **5**, there is one O–H···O type of hydrogen bond interaction between the solvent methanol and the main compound, O1S–H1S to O1, where 'S' refers to the solvent. In the case of **8**, the lattice acetic acid forms three hydrogen bonds with two different molecules of **8**, in which two are of the C–H···O type while the third one is of O···H···O type. The molecule also forms intermolecular hydrogen bonds through C–H···O types of interaction.

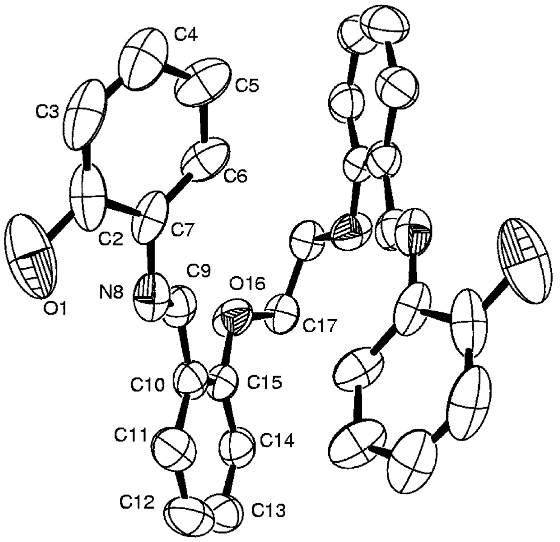

Fig. 4 ORTEP drawing for the molecular structure of H_2L^3. The molecule sits on a center of symmetry.

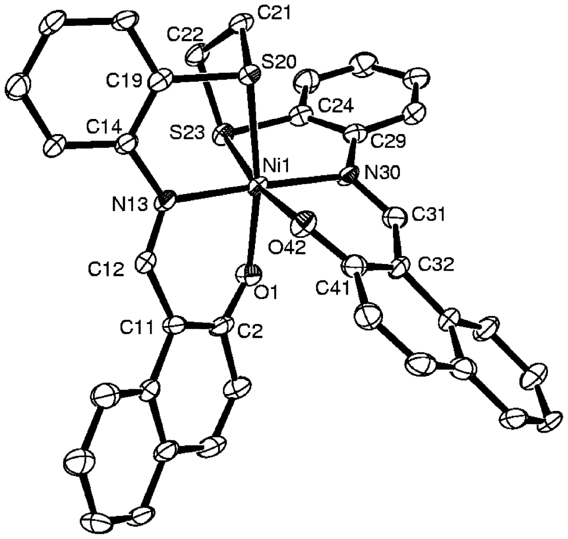

Fig. 6 Molecular structure for **5** as an ORTEP plot.

4. Reactions of H_2L^1–H_2L^3 with Zn(II)

The products **3**, **6** and **9** are obtained by reacting $Zn(CH_3COO)_2{\cdot}2H_2O$ with H_2L^1, H_2L^2 and H_2L^3, respectively. The product formulations were supported by the observed satisfactory elemental analysis data as well as the molecular weight obtained through the molecular ion peak in the FAB mass spectra. For these diamagnetic Zn(II) complexes, the ^1H NMR spectra exhibited peaks corresponding to half of the ligand, suggesting retention of the ligand symmetry even in the bound state. The ^1H NMR peaks arising from the $–S–CH_2–CH_2–S–$ moiety in the case of **3** and **6** are found to be overlapped by the broad peak arising from water in DMSO-d_6. On the other hand the peak arising from $–O–CH_2–CH_2–O–$ in **9** was observed at 4.384 ppm. Disappearance of the peak due to phenolic –OH and an upfield shift observed in the peak for the –CH=N proton both indicate that the Zn(II) is bound through the azomethine and phenolic groups in **3**, **6** and **9**.

Molecular structures of 3, 6 and 9. Lattices of **6** and **9** have a center of symmetry. From the crystal structures of all three Zn(II) complexes it was observed that neither the C–S nor C–O bond is cleaved. The ORTEP structure for **9** is shown in Fig. 7. In all three structures the corresponding ligand acts as a doubly negative one and extends six coordinating sites to the Zn(II) center, resulting in neutral mononuclear complexes. All three complexes have highly distorted octahedral Zn(II) centers, as can be judged from the spread in their observed bite angles and *trans* angles: 79.0(1)°–104.3(1)° and 162.6(1)°, 165.3(2)° and 168.2(1)° in the case of **3**; 77.6(1)°–103.0(1)° and 162.8(1)°, 162.8(1)° and 166.3(1)° for **6**; 74.4(1)°–111.6(1)° and 156.6(1)°, 156.6(1)° and 168.1(1)° in the case of **9**. Among the three complexes, the Zn(II) center in **9** with an N_2O_4 core is more distorted than in **3** and **6** having an $N_2O_2S_2$ core. In all cases both nitrogen atoms are disposed *trans* to each other. The conformation of the three 5-membered and two 6-membered chelate rings formed by the Zn(II) center in each case is given in Table 1 and selected bond angles in the coordination sphere are given in Table 3.

The bond lengths observed in **9**, $Zn–O_{ether}$ = 2.328(2), $Zn–O_{phenolic}$ = 2.020(2) and Zn–N = 2.151(2) Å, are quite normal when compared with the corresponding distances reported in the literature and the metric parameters fit well with an octahedral geometry around the Zn(II) center. The observed $Zn–O_{ether}$ distances in the present case are well within the range reported

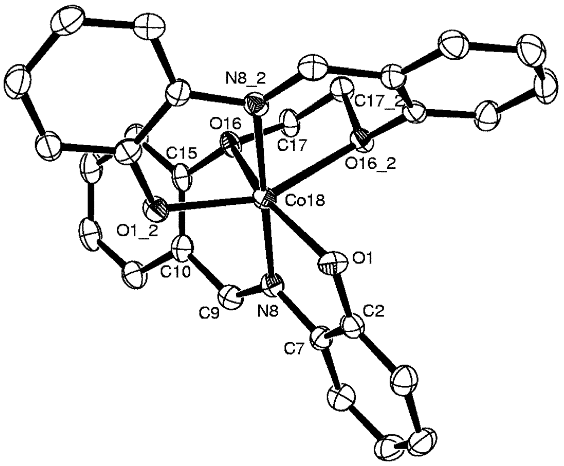

Fig. 5 Molecular structure for **7** as an ORTEP plot. Co(II) sits on a center of symmetry.

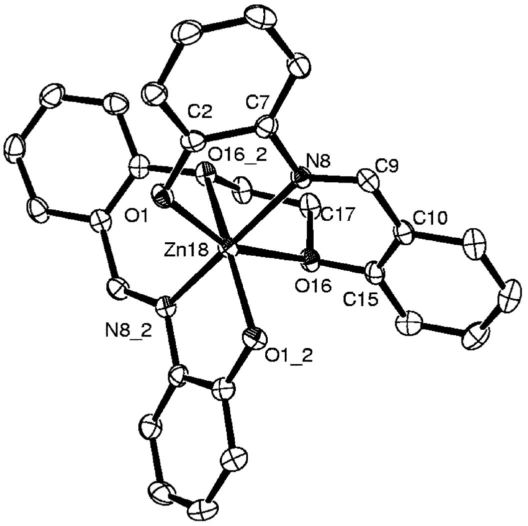

Fig. 7 Molecular structure for **9** as an ORTEP plot. Zn(II) sits on a center of symmetry.

for a Zn(II)-crown ether complex (2.34–2.60 Å).[5a] Recently, we reported a weak interaction of the pyranose oxygen with the Zn(II) center, resulting in a Zn–O distance of 2.759 Å.[5b]

On the other hand, in the case of **3** and **6** the bond lengths, Zn–$O_{phenolic}$ = 1.978(2)–2.009(1) Å and Zn–N = 2.073(1)–2.101(1) Å, are well within the covalent bond distances for the corresponding pairs, while the Zn–S distances are in the range of 2.582(1)–2.692(1) Å, well within the sum of the van der Waals radii. In the literature, the Zn–S distances in thiolates are observed to be around 2.300–2.360 Å for terminal bonds and 2.400–2.450 Å for bridging ones.[5c] The Zn–S distances observed in the present case are somewhat longer than that observed in the crown thioether (2.497 Å) and shorter than that observed in the complex of dithiaalkyl-substituted triazine 1-oxide (2.649–2.720 Å).[5d,1c] The Zn(II) exhibits pseudo-octahedral geometry. However, when these two Zn–S interactions are disregarded the resulting ZnN_2O_2 core does not fit well with a tetrahedral geometry, strongly suggesting that the coordination sphere is more of a distorted octahedral rather than tetrahedral. The selected bond lengths of the coordination sphere are given in Table 2.

Conclusions and comparisons

The complexes of Co(III), Co(II), Ni(II) and Zn(II) with H_2L^1–H_2L^3 reported in this paper are all neutral and found to have distorted octahedral geometries, however, **3** and **6** have a pseudo-octahedral geometry. The present study clearly demonstrates the formation of two tridentate ligands from the precursor hexadentate ligands ($N_2O_2S_2$, H_2L^1 and H_2L^2) *via* C–S bond cleavage as a result of the oxidation of Co(II). Such C–S bond cleavage was found to occur with the Co(II) salts of chloride, sulfate, acetate and acetylacetonate. On the other hand, H_2L^3, possessing a N_2O_4 core, does not exhibit cleavage of the C–O bond under the same conditions. On going from Co(III) (**1**) to the Co(II) (**7**) complex, the corresponding bond lengths in the primary coordination sphere are considerably increased, consistent with the change in the oxidation state of cobalt.

To observe the role of the metal ion, we extended these studies using Ni(II) and Zn(II) salts. Combining the present studies with what is known in the literature, the following aspects are relevant for bond cleavage: (a) the presence of 'S' instead of 'O', (b) the metal ion should support various oxidation states and (c) the thioether chelate should be 5-membered.

In all the complexes the two imine nitrogens are *trans*- to each other. On going from a trivalent complex (**1**, Co^{3+}) to divalent complexes (Co^{2+}: **7**; Ni^{2+}: **5** and **8**; Zn^{2+}: **3**, **6** and **9**) the primary coordination distances, *viz.*, M–N, M–$O_{phenolate}$ or M–S, generally increase by 0.1 Å or more owing to the change in size of the corresponding metal ion center. These distances increase further in the case of the Zn^{2+} complexes as compared to the Ni^{2+} or Co^{2+} complexes, owing to expansion of the coordination sphere of Zn^{2+} from its commonly observed tetrahedral geometry to the pseudo-octahedral one.

The Co(II), Ni(II) and Zn(II) complexes derived from H_2L^3 are more distorted than the Co(III), Ni(II) and Zn(II) complexes derived from the other two ligands, *viz.*, H_2L^1 and H_2L^2. The extent of distortion observed about the metal ion coordination sphere in these complexes follows a trend, Zn(II) > Co(II) > Ni(II), as can be deduced from the corresponding bond lengths and bond angles. This can also be seen from the stereo views of the complexes **7**, **8** and **9** given in Fig. 8. Among all the complexes, **1** with Co(III) has the least distortion due to cleavage of the hexadentate ligand into two tridentate ligands.

The conformation of the 5-membered rings can be half chair (C_2), envelope (C_s) or planar (A), while the six-membered rings exhibit boat or skew boat conformations.

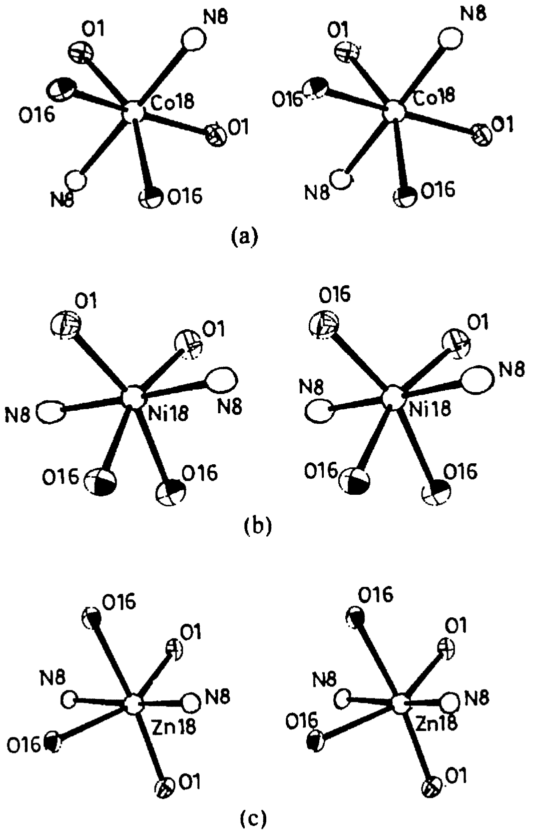

Fig. 8 Stereo views of the primary coordination spheres for the complexes (a) **7** (CoN_2O_4), (b) **8** (NiN_2O_4) and (c) **9** (ZnN_2O_4).

Experimental details

General remarks

1,2-Dibromoethane was procured from Spectrochem Pvt. Ltd.; *o*-hydroxynapthaldehyde and 1,2-di(2-aminophenylthio)-ethane were synthesized as per the reported procedures.[6a,6b] Ethylene-2-2′-(dioxydibenzaldehyde) was synthesized as per the reported procedure but with some modifications.[6c] All the solvents were purified and dried immediately before use. Elemental analysis was carried out on a CE Instruments Flash EA 1112 series apparatus; FTIR spectra were recorded on Nicolet Magna IR 550; UV-Vis spectra were recorded on a UV-2101PC spectrophotometer. FAB mass spectra were recorded on a JEOL SX 102/DA-6000 mass spectrometer data system using argon–xenon (6 kV, 10 mA) as the FAB gas. The accelerating voltage was 10 kV and the spectra were recorded at room temperature with *m*-nitrobenzyl alcohol (NBA) as the matrix. GC-mass spectra were recorded on a 5989 B MS engine model from Hewlett Packard. ^1H NMR spectra were recorded on a Varian VXR 300S. ^{13}C spectra were recorded on a Bruker Avance DRX 500 spectrometer.

Syntheses

Ethylene-2-2′-(dioxydibenzaldehyde). A solution of sodium hydroxide (11.25 g, 279 mmol) in water (78 ml) was slowly added over a period of 30 min to a mixture of salicylaldehyde (30.53 g, 250 mmol) and 1,2-dibromoethane (72.8 g, 387 mmol) at its boiling point. After an additional 20 h of boiling, the reaction mixture was cooled to room temperature. The organic phase was separated and the aqueous phase was extracted with dichloromethane (2 × 40 ml), then combined with the original organic phase. The organic layer was then washed with 10% sodium hydroxide (20 ml) and dried over $MgSO_4$. The dichloromethane was removed by rotary evaporation and the resulting residue was cooled at 4 °C overnight. The solid thus separated was filtered and was washed with diethyl ether and then dried under vacuum. The colorless solid was further crystallized from acetone or hot petroleum ether (5.5 g, 16%). M.p. 110–112 °C. ^{1}H-NMR (300 MHz, CDCl$_3$) δ: 4.520 (s, 4H, –OCH$_2$CH$_2$O–), 7.031–7.842 (m, 8H, aromatic H), 10.412 (s, 2H, –CH=O). FTIR (KBr) υ/cm^{-1}: 2946, 2866, 1687, 1597, 1485, 1452, 1242, 1061, 834, 754. GC-MS *m*/*z*: 270 [M]$^{+}$. Anal. found: C 70.89, H 4.97%; calcd for $C_{16}H_{14}O_4$: C 71.10, H 5.22%.

1,2-Di(salicylaldimino-*o*-phenylthio)ethane, H$_2$L^1. This ligand was synthesized in 85% yield as per the procedure reported earlier.[3a] The compound was crystallized from a mixture of CHCl$_3$ and EtOH and the structure was established by single crystal XRD. M.p. 189–190 °C. ^{1}H-NMR (300 MHz, [D6]DMSO) δ: 3.207 (s, 4H, –SCH$_2$CH$_2$S–), 6.948–7.663 (m, 16H, aromatic H), 8.913 (s, 2H, –CH=N), 12.984 (s, 2H, –OH). ^{13}C-NMR (300 MHz, [D6]DMSO) δ: 30.6 (–SCH$_2$CH$_2$S–), 163.0 (–CH=N), 116.6–160.2 (aromatic C). FTIR (KBr) υ/cm^{-1}: 3000, 1612, 1573, 1561, 1468, 1279, 1181, 907, 753. UV-Vis (CH$_2$Cl$_2$) $\lambda_{\max}$/nm (ε/mol^{-1} L cm^{-1}): 351 (26 900), 272 (52 100), 234 (54 800). FAB-MS *m*/*z*: 485 [M]$^{+}$ (70%). Anal. found: C 69.82, H 4.91, N 5.38, S 12.74%; calcd for $C_{28}H_{24}N_2O_2S_2$: C 69.39, H 4.99, N 5.78, S 13.23%.

1,2-Di(naphthaldimino-*o*-phenylthio)ethane, H$_2$L^2. This ligand was synthesized by adopting the procedure used for H$_2$L^1 but with *o*-hydroxynapthaldehyde in place of salicylaldehyde (2.8 g, 95%). M.p. 198–200 °C. ^{1}H-NMR (300 MHz, [D6]DMSO) δ: 3.195 (s, 4H, –SCH$_2$CH$_2$S–), 7.023–8.522 (m, 20H, aromatic H), 9.630 (s, 2H, –CH=N), 15.384 (s, 2H, –OH). ^{13}C-NMR (300 MHz, [D6]DMSO) δ: 30.0 (–SCH$_2$CH$_2$S–), 155.9 (–CH=N), 118.4–136.3 (aromatic C). FTIR (KBr) υ/cm^{-1}: 3400, 1620, 1553, 1460, 1326, 1168, 816, 743. UV-Vis (DMSO) $\lambda_{\max}$/nm (ε/mol^{-1} L cm^{-1}): 471 (18 900), 439 (25 700), 398 (36 800), 320 (35 700). FAB-MS *m*/*z*: 585 [M]$^{+}$ (100%). Anal. found: C 73.07, H 4.66, N 4.64%; calcd for $C_{36}H_{28}N_2O_2S_2$: C 73.95, H 4.83, N 4.79%.

1,2-Di(*O*-salicylaldimino-*o*-hydroxyphenyl)ethane, H$_2$L^3. A 25 ml ethanolic solution containing ethylene-2-2’-(dioxydibenzaldehyde) (1.25 g, 4.629 mmol) and *o*-aminophenol (1.07 g, 9.820 mmol) was refluxed for 6 h; then the contents of the flask were cooled to room temperature, yielding yellow-colored needles suitable for single crystal XRD (1.78 g, 85%). M.p. 122–124 °C. ^{1}H-NMR (300 MHz, CDCl$_3$) δ: 4.519 (s, 4H, –OCH$_2$CH$_2$O–), 6.737–8.145 (m, 16H, aromatic H), 9.083 (s, 2 H, –CH=N). FTIR (KBr) υ/cm^{-1}: 3423, 1619, 1593, 1489, 1449, 1374, 1221, 1047, 748. UV-Vis (DMSO) $\lambda_{\max}$/nm (ε/mol^{-1} L cm^{-1}): 391 (16 750), 354 (36 800), 323 (30 050). FAB-MS *m*/*z*: 453 [M]$^{+}$ (65%). Anal. found: C 73.90, H 5.06, N 5.74%; calcd for $C_{28}H_{24}N_2O_4$: C 74.32, H 5.35, N 6.19%.

[Co(III)(L^{1a})(L^{1b})], 1. To a CH$_2$Cl$_2$–CH$_3$OH (9.5:0.5 v/v) solution of H$_2$L^1 (0.480 gm, 0.989 mmol), Co(CH$_3$COO)$_2$·4H$_2$O (0.253 gm, 1.02 mmol) was initially allowed to react under Ar atmosphere and then followed by purging O$_2$ for 8 h. During this time, the reaction mixture went through a color change from orange red to dark brown. The reaction mixture was filtered. The residue was washed with diethyl ether and dried *in vacuo*. The filtrate was layered with diethyl ether to get dark brown colored crystals suitable for single crystal XRD (0.470 g, 86%). M.p. > 250 °C. ^{1}H-NMR (300 MHz, [D$_6$]DMSO) δ: 5.572–5.889 (s, 3H, –SCH=CH2), 6.423–8.476 (m, 16H, aromatic H), 8.805 (s, 1H, –CH=N), 8.934 (s, 1H, –CH=N). ^{13}C-NMR (300 MHz, [D6]DMSO) δ: 159.4 (–CH=N), 162.2 (–CH=N), 113.5–166.0 (aromatic C and –CH=CH$_2$). FTIR (KBr) υ/cm^{-1}: 1604, 1573, 1519, 1525, 1435, 1249, 1177, 1143, 927, 747. UV-Vis (DMSO) $\lambda_{\max}$/nm (ε/mol^{-1} L cm^{-1}): 475 (10 800), 440 (10 700), 285 (57 800). FAB-MS *m*/*z*: 541 [M]$^{+}$ (85%). Anal. found: C 62.32, H 3.75, N 5.00, S 11.31%; calcd for $C_{28}H_{21}CoN_2O_2S_2$: C 62.22, H 3.92, N 5.18, S 11.86%.

[Ni(L^1)], 2. To a CH$_2$Cl$_2$–CH$_3$OH (9.5:0.5 v/v) solution of H$_2$L^1 (0.485 gm, 1 mmol), Ni(CH$_3$COO)$_2$·4H$_2$O (0.249 gm, 1 mmol) was added and the mixture stirred for 6 h. The clear solution resulting at the end was layered with diethyl ether to get dark red colored crystals (0.300 g, 55%). M.p. > 250 °C. FTIR (KBr) υ/cm^{-1}: 1604, 1570, 1518, 1438, 1388, 1139, 755. UV-Vis (DMSO) $\lambda_{\max}$/nm (ε/mol^{-1} L cm^{-1}): 879 (26), 567 (142), 455 (9300), 309 (10 040). FAB-MS *m*/*z*: 541 [M]$^{+}$ (100%). Anal. found: C 61.73, H 3.89, N 4.95%; calcd for $C_{28}H_{22}NiN_2O_2S_2$: C 62.13, H 4.10, N 5.18%.

[Zn(L^1)], 3. This complex was synthesized by adopting the procedure used for **2**, with Zn(CH$_3$COO)$_2$·2H$_2$O (0.220 gm, 1 mmol) in place of nickel acetate. The clear solution was concentrated to give bright yellow-colored crystals (0.220 g, 40%). M.p. > 250 °C. ^{1}H-NMR (300 MHz, [D$_6$]DMSO) δ: 6.364–7.682 (m, 16H, aromatic H), 8.708 (s, 2H, –CH=N). FTIR (KBr) υ/cm^{-1}: 1611, 1560, 1465, 1370, 1276, 1180, 752. FAB-MS *m*/*z*: 548 [M]$^{+}$ (15%). Anal. found: C 61.10, H 4.29, N 5.25%; calcd for $C_{28}H_{22}N_2O_2S_2Zn$: C 61.37, H 4.05, N 5.11%.

[Co(III)(L^{2a})(L^{2b})], 4. This complex was synthesized by adopting the procedure used for **1**, with H$_2$L^2 (0.580 gm, 0.991 mmol) in place of H$_2$L^1. The reaction mixture was filtered and the filtrate was layered with diethyl ether to get the dark brown colored solid, which was dried *in vacuo* (0.500 g, 79%). M.p. > 200 °C. ^{1}H-NMR (300 MHz, [D$_6$]DMSO) δ: 5.574–5.957 (s, 3H, –SCH=CH$_2$), 6.621–8.583 (m, 20H, aromatic H), 9.347 (s, 1H, –CH=N), 9.384 (s, 1H, –CH=N). ^{13}C-NMR (300 MHz, [D6]DMSO) δ: 126.9 (–SCH=CH$_2$), 128.8 (– SCH=CH$_2$), 153.0 (–CH=N), 155.3 (–CH=N), 115–137 (aromatic C). FTIR (KBr) υ/cm^{-1}: 1600, 1572, 1532, 1515, 1423, 1385, 1183, 747. UV-Vis (DMSO) $\lambda_{\max}$/nm (ε/mol^{-1} L cm^{-1}): 510 (15 500), 480 (20 100), 446 (17 100), 341 (33 700), 284 (88 400). FAB-MS *m*/*z*: 641 [M]$^{+}$ (100%). Anal. found: C 67.15, H 3.86, N 4.15%; calcd for $C_{36}H_{25}CoN_2O_2S_2$: C 67.50, H 3.93, N 4.37%.

[Ni(L^2)], 5. This compound was synthesized by adopting the procedure used for **2** with H$_2$L^2 (0.585 gm, 1 mmol) and Ni(CH$_3$COO)$_2$·4H$_2$O (0.249 gm, 1 mmol). The clear reaction mixture was layered with diethyl ether to yield dark red colored crystals (0.385 g, 60%). M.p. > 250 °C. FTIR (KBr) υ/cm^{-1}: 1608, 1569, 1530, 1389, 1266, 1177, 828, 747. UV-Vis (DMSO) $\lambda_{\max}$/nm (ε/mol^{-1} L cm^{-1}): 881 (66), 599 (276), 471 (56 700), 445 (43 800), 334 (46 500), 279 (91 400). FAB-MS *m*/*z*: 641 [M]$^{+}$ (100%). Anal. found: C 66.93, H 4.37, N 3.97%; calcd for $C_{36}H_{26}NiN_2O_2S_2$: C 67.41, H 4.09, N 4.37%.

[Zn(L^2)], 6. This compound was synthesized by adopting the procedure used for **2** using H$_2$L^2 (0.585 gm, 1 mmol) and Zn(CH$_3$COO)$_2$·2H$_2$O (0.220 gm, 1 mmol). The clear reaction mixture obtained was concentrated to give bright yellow-colored crystals (0.290 g, 48%). M.p. > 250 °C. ^{1}H-NMR (300 MHz, [D$_6$]DMSO) δ: 6.566–8.229 (m, 20H, aromatic H), 9.363 (s, 2H, –CH=N). FTIR (KBr) υ/cm^{-1}: 1608, 1567, 1531, 1394, 1362, 1177, 832, 747. FAB-MS *m*/*z*: 648 [M]$^{+}$ (85%). Anal. found: C 66.90, H 3.90, N 4.15%; calcd for $C_{36}H_{26}N_2O_2S_2Zn$: C 66.72, H 4.04, N 4.32%.

[Co(L^3)], 7. To a CH$_2$Cl$_2$–CH$_3$OH (20:10 v/v) solution of H$_2$L^3 (0.894 gm, 1.974 mmol), Co(CH$_3$COO)$_2$·4H$_2$O (0.523

Table 4 Summary of crystallographic data for H_2L^1, H_2L^3, **1**, **3**, **5**, **6**, **7**, **8** and **9**

Compounds	H_2L^1	H_2L^3	**1**	**3**	**5**	**6**	**7**	**8**	**9**
Empirical formula	$C_{28}H_{24}N_2O_2S_2$	$C_{14}H_{12}NO_2$	$C_{28}H_{21}CoN_2O_2S_2$	$C_{28}H_{22}N_2O_2S_2Zn$	$C_{36.5}H_{28}N_2O_{2.5}S_2Ni$	$C_{18}H_{13}NOS\ Zn_{0.5}$	$C_{16}H_{15}Co_{0.50}NO_4$	$C_{16}H_{15}Ni_{0.5}O_4$	$C_{15}H_{15}NO_3Zn_{0.5}$
Formula weight	484.61	226.25	540.52	547.97	657.44	648.08	314.75	314.64	289.96
T/K	173(2)	173(2)	150(2)	173(2)	173(2)	173(2)	173(2)	173(2)	173(2)
Crystal system	Monoclinic	Orthorhombic	Monoclinic	Tetragonal	Triclinic	Monoclinic	Tetragonal	Tetragonal	Tetragonal
Space group	$P2_1/c$	$Pbcn$	Cc	$P4_1$	$P1$	$C2/c$	$P4_2/n$	$P4_2/n$	$P4_2/n$
a/Å	10.716(1)	17.254(1)	15.279(1)	11.383(1)	10.750(1)	22.994(1)	13.929(2)	13.925(2)	13.925(2)
b/Å	16.811(1)	8.395(1)	12.807(1)	11.383(1)	12.299(1)	7.612(1)	13.929(2)	13.925(2)	13.925(2)
c/Å	13.097(1)	15.994(1)	12.191(1)	18.347(1)	12.656(1)	17.980(2)	14.231(1)	14.181(3)	14.181(3)
α/°					84.38(1)				
β/°	104.23(1)		94.51(1)		67.41(1)	110.55(1)			
γ/°					70.99(1)				
U/Å^3)	2287.0(3)	2316.7(1)	2378.1(3)	2377.3(3)	1460.0(2)	2946.8(5)	2761.1(1)	2749.8(8)	2749.8(8)
Z	4	8	4	4	2	4	8	8	8
μ/mm^{-1}	0.263	0.087	0.927	1.239	0.848	1.012	0.680	0.765	0.939
Reflections collected	12 704	9192	6743	8877	5901	4626	17 104	18 110	17 541
Independent reflections	4014	1496	3542	3546	4324	2501	2620	2594	2496
R_{int}	0.0281	0.0501	0.0317	0.0485	0.0357	0.0311	0.1015	0.1233	0.1048
R_1 [$I > 2\sigma(I)$]	0.0634	0.0660	0.0276	0.0375	0.0507	0.0339	0.0439	0.0746	0.0382
wR_2 [$I > 2\sigma(I)$]	0.1619	0.1532	0.0624	0.072	0.1099	0.0664	0.0924	0.1695	0.0708
R_1 (all data)	0.0744	0.0939	0.0303	0.0477	0.0750	0.0529	0.0787	0.1044	0.0756
wR_2 (all data)	0.1712	0.1711	0.0636	0.0737	0.1229	0.0726	0.1060	0.1863	0.0818

gm, 2.1 mmol) was added; O_2 was purged into the reaction mixture while stirring for 6 h. The residue was filtered and the filtrate was concentrated to give red-colored crystals (0.900 g, 80%). M.p. > 200 °C. FTIR (KBr) υ/cm^{-1}: 1598, 1583, 1469, 1390, 1305, 1284, 1141, 734. UV-Vis (DMSO) λ_{max}/nm (ε/mol^{-1} L cm^{-1}): 446 (26 700), 312 (33 700). FAB-MS m/z: 509 [M]$^+$ (10%). Anal. found: C 65.90, H 4.43, N 5.25%; calcd for $C_{28}H_{22}CoN_2O_4$: C 66.02, H 4.35, N 5.50%.

[Ni(L^3)], 8. To a CH_2Cl_2–CH_3OH (20:10 v/v) solution of H_2L^3 (0.880 gm, 1.943 mmol), $Ni(CH_3COO)_2{\cdot}4H_2O$ (0.530 gm, 2.129 mmol) was added and the mixture stirred for 6 h. The residue was filtered and the filtrate concentrated to give dark red colored crystals (0.750 g, 76%). M.p. > 200 °C. FTIR (KBr) υ/cm^{-1}: 1600, 1583, 1469, 1279, 1241, 742, 500. UV-Vis (DMSO) λ_{max}/nm (ε/mol^{-1} L cm^{-1}): 908 (50), 624 (230), 471 (33 950), 343 (19 600), 314 (36 350). FAB-MS m/z: 509 [M]$^+$ (45%). Anal. found: C 65.54, H 4.81, N 5.06%; calcd for $C_{28}H_{22}NiN_2O_4$: C 66.05, H 4.36, N 5.50%.

[Zn(L^3)], 9. To a CH_2Cl_2–CH_3OH (20:10 v/v) solution of H_2L^3 (0.900 gm, 1.987 mmol), $Zn(CH_3COO)_2{\cdot}2H_2O$ (0.470 gm, 2.136 mmol) was added and the mixture stirred for 6 h. The reaction mixture was filtered and the filtrate was concentrated and layered with diethyl ether to give a dark yellow-colored solid. This was separated by filtration and the residue was washed with diethyl ether. The compound was recrystallised from methanol to give bright yellow-colored crystals suitable for a single crystal XRD study (0.719 g, 70%). M.p. 175–80 °C. ^{1}H-NMR (300 MHz, [D$_6$]DMSO) δ: 4.384 (s, 4H, –OCH_2CH_2O–), 6.293–7.778 (m, 16H, aromatic H), 8.774 (s, 2H, –CH=N). FTIR (KBr) υ/cm^{-1}: 1598, 1486, 1451, 1290, 1256, 752. FAB-MS m/z: 516 [M]$^+$ (40%). Anal. found: C 64.89, H 4.34, N 5.29%; calcd for $C_{28}H_{22}N_2O_4Zn$: C 65.19, H 4.30, N 5.43%.

Structure determination

Single crystal X-ray diffraction data were collected for all the compounds on a Nonius Kappa CCD diffractometer in the ϕ scan + ω scan mode using Mo-K$_\alpha$ of wavelength 0.71073 Å. All the structures were solved using direct methods with SIR-92 (H_2L^1 and **3**) and SHELXS-97 (H_2L^3, **1**, **5**, **7**, **8** and **9**) and were refined using the SHELXL-97 program.[7,8] The diagrams were generated using ORTEP3.[9] Full-matrix least-squares refinement with anisotropic thermal parameters for all non-hydrogen atoms was used. In case of the ligand structures, –OH hydrogen positions were recovered from the difference Fourier map. The hydrogen atoms were treated as riding atoms with fixed thermal parameters. The empirical absorption correction was applied in the case of **1** and **3**. In other structures there was no absorption correction employed. The crystals are found to be stable and other details of data collection and structure refinement are provided in Table 4.†

Acknowledgements

CPR acknowledges financial support from the Council of Scientific and Industrial Research (CSIR), New Delhi, and the Department of Science and Technology, New Delhi. GR acknowledges an SRF fellowship from CSIR.

References

1 (*a*) S. Zhou, S. Liu and Z. Zhou, *Huaxue Shiji*, 2001, **23**, 26; (*b*) S. Pal, S. Ghosh, G. Mukherjee and A. K. Nandi, *Polyhedron*, 1998, **17**, 3439; (*c*) P. Chakraborty, S. K. Chandra and A. Chakravorty, *Inorg. Chim. Acta*, 1995, **229**, 477; (*d*) P. Chattopadhyay and C. Sinha, *Indian J. Chem., Sect. A: Inorg., Bio-inorg., Phys., Theor.*

---

† CCDC reference numbers: 172 099 (H_2L^1, EGEXIX), 216 935 (H_2L^3), 172 100 (**1**, EGIXIB), 195 200 (**3**, EGIXOH), 216 930 (**5**), 216 931 (**6**), 216 932 (**7**), 216 933 (**8**) and 216 934 (**9**). See http://www.rsc.org/suppdata/nj/b3/b305313j/ for crystallographic data in .cif or other electronic format.

Anal Chem., 1995, **76**, 34; (*e*) K. Dey, D. Bandyopadhyay, K. K. Nandi, S. N. Poddar, G. Mukhopadhyay and G. B. Kauffman, *Synth. React. Inorg. Met.-Org. Chem.*, 1992, **22**, 1111; (*f*) E. F. W. Thurston, *J. Photogr. Sci.*, 1990, **38**, 34; (*g*) H. P. Nur, M. T. Rahman and A. Malek, *Inorg. Nucl. Chem. Lett.*, 1981, **17**, 133; (*h*) N. E. MacKenzie, R. H. Thomson and C. W. Greenhalgh, *J. Chem. Soc., Perkin Trans. 1*, 1980, **12**, 2923; (*i*) K. Motoda, H. Sakiyama, N. Matsumoto, H. Okawa and D. E. Fenton, *J. Chem. Soc., Dalton Trans.*, 1995, **20**, 3419; (*j*) P. Comba, A. Fath, T. W. Hambley, A. Kühner, D. T. Richens and A. Vielfort, *Inorg. Chem.*, 1998, **37**, 4389; (*k*) W.-X. Zhang, C. Ma and S. Si, *Transition Met. Chem.*, 2001, **26**, 380.

2 G. Rajsekhar, C. P. Rao, P. K. Saarenketo, E. Kolehmainen and K. Rissanen, *Inorg. Chem. Commun.*, 2002, **5**, 649.

3 (*a*) R. D. Cannon, B. Chiswell and L. M. Venanzi, *J. Chem. Soc. A*, 1967, **8**, 1277; (*b*) F. P. Dwyer, N. S. Gill, E. C. Gyarfas and F. Lions, *J. Am. Chem. Soc.*, 1954, **76**, 383; (*c*) G. Mukherjee, S. P. Poddar and K. Dey, *Indian J. Chem., Sect. A: Inorg., Bioinorg., Phys., Theor. Anal Chem.*, 1986, **275**, 25; (*d*) G. Mukherjee, S. P. Poddar, K. Choudhury and K. Dey, *Transition Met. Chem.*, 1988, **13**, 58.

4 (*a*) K. Umakoshi, T. Yamasaki, A. Fukuoka, H. Kawano, M. Ichikawa and M. Onishi, *Inorg. Chem.*, 2002, **41**, 4093; (*b*) X. Fan, R. Cao, M. Hong, W. Su and D. Sun, *J. Chem. Soc., Dalton Trans.*, 2001, **20**, 2961; (*c*) T. Arliguie, C. Lescop, L. Ventelon, P. C. Leverd, P. Thuery, M. Nierlich and M. Ephritikhine, *Organometallics*, 2001, **20**, 3698; (*d*) G. E. M. Mullen, P. J. Blower, D. P. Price, A. K. Powell, M. J. Howard and M. J. Went, *Inorg. Chem.*, 2000, **39**, 4093; (*e*) T. Morikita, M. Hirano, A. Sasaki and S. Komiya, *Inorg. Chim. Acta.*, 1999, **291**, 341; (*f*) L. R. Hanton and K. Lee, *Inorg. Chem.*, 1999, **38**, 1634; (*g*) M. Hong, W. Su, R. Cao, F. Jiang, H. Liu and J. Lu, *Inorg. Chim. Acta*, 1998, **274**, 229; (*h*) J. G. Planas, M. Hirano and S. Komiya, *Chem. Lett.*, 1998, **2**, 123; (*i*) P. Chakroborty, S. K. Chandra and A. Chakravorty, *Inorg. Chem.*, 1994, **33**, 4959 and references cited therein; (*j*) S. Y. Darensbourg, *Heterolytic and homolytic S–C bond cleavage reactions in nickel thioether complexes*, Book of Abstracts, 211th ACS National Meeting, New Orleans, LA, 1996; (*k*) P. Chakraborty, S. Karmakar, S. K. Chandra and A. Chakravorty, *Inorg. Chem.*, 1994, **33**, 816; (*l*) P. Chakraborty, S. K. Chandra and A. Chakravorty, *Organometallics*, 1993, **12**, 4726.

5 (*a*) A. B. Charette, J. F. Marcoux and F. Belanger-Gariepy, *J. Am. Chem. Soc.*, 1996, **118**, 6792; (*b*) A. K. Sah, C. P. Rao, E. K. Wegelius, E. Kolehmainen and K. Rissanen, *Carbohydr. Res.*, 2001, **336**, 249; (*c*) A. D. Watson, C. P. Rao, J. R. Dorfman and R. H. Holm, *Inorg. Chem.*, 1985, **24**, 2820; (*d*) M. L. Helm, C. M. Combs, D. G. VanDerveer and G. J. Grant, *Inorg. Chim. Acta*, 2002, **338**, 182.

6 (*a*) J. C. Duff and E. J. Bills, *J. Chem. Soc.*, 1934, 1305; (*b*) R. W. Hay, P. M. Gidney and G. A. Lawrance, *J. Chem. Soc., Dalton Trans.*, 1975, 779; (*c*) P. A. Duckworth, F. S. Stephens, K. P. Wainwright, K. D. V. Weerasuria and S. B. Wild, *Inorg. Chem.*, 1989, **28**, 4531.

7 SIR-92: A program for crystal structure solution. A. Altomore, G. Cascarano, C. Giacovazzo and A. Guagliardi, *J. Appl. Crystallogr.*, 1993, **26**, 343.

8 G. M. Sheldrick, *SHELX-97 Programs for Crystal Structure Analysis (Release 97-2)*, University of Göttingen, Germany, 1998.

9 L. J. Farrugia, *J. Appl. Crystallogr.*, 1997, **30**, 565.